SIMULTANEOUS DYNAMIC COMPENSATION OF STOPBANDS AND
MULTIPURPOSE LOCATION OF CORRECTION LENSES IN THE CERN PS BOOSTER

K. Schindl*

Abstract and Introduction

Three 3rd order stopbands, amongst them the structural $3Q_V = 16$ (= number of lattice periods), are compensated simultaneously for the first 100 msec of the acceleration cycle. The location of the correction multipoles was optimized for all relevant resonance harmonics. The ultimate Q_H-Q_V working area still being uncertain, all stopbands up to order four as well as 3rd order crossing point were considered when choosing the locations of the new sextupoles and octupoles, eight per type and ring. A solution providing ideal locations for pairs of lenses applying to almost all harmonics was found. Experiments dealing with compensation of $3Q_V = 16$ are described. With simultaneous dynamic correction of $2Q_H + Q_V = 14$, $Q_H + 2Q_V = 15$ and $3Q_V = 16$, high intensity beams of a transverse density hitherto unknown in the PS Booster were obtained.

Working points, Q-shift, stopbands concerned

With 100 mA from the new linac[1], 1.8×10^{13} ppp have been accelerated from 50 to 800 MeV in the four-ring PS Booster (PSB). The betatron tunes are moved from $(Q_H, Q_V) = (4.23, 5.31)$ towards $(4.17, 5.23)$ during the 0.6 s acceleration cycle, thus steering clear between two limiting phenomena[2] (Fig. 1): i) particles are swept over $Q_V = 5$ owing to an incoherent Q-shift of > 0.5, giving rise to a doubling of vertical emittance (ε_V) and to filling eventually the vertical PSB acceptance (70 π μradm); ii) almost complete beam destruction on $3Q_V = 16$. The present "low" working point is hence a likely major obstacle to higher PSB beam density. The alternatives to avoid this restriction are: i) to move to another working area; ii) to employ a "high" dynamic working point in the present area (Fig. 1). Exploratory studies[3] have shown so far that, in spite of $3Q_V = 16$, the present area appears best suited to accommodate the beam; the combined effect of resonances of order 1 to 4 eliminates all other areas investigated. Alternative (ii) entails simultaneous compensation of at least $2Q_H + Q_V = 14$, $Q_H + 2Q_V = 15$, $3Q_V = 16$, for the first 100 ms from injection.
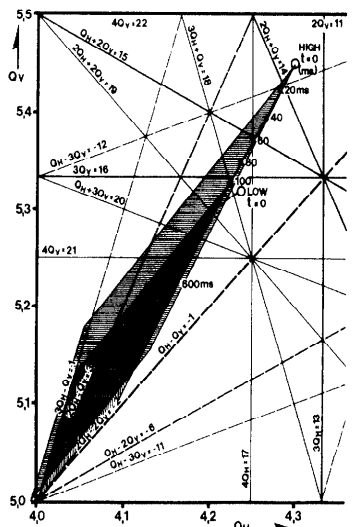

Fig. 1 Dynamic working points and Q-shift (at 0, 100, 600 ms after injection) in the PSB (5×10^{12} pp ring).

*PS Division, CERN, Geneva, Switzerland.

Although experiments showed[2,4] that crossing the natural 4th order stopbands is barely detrimental to beam quality, they are nevertheless considered in what follows on account of side effects generated by the Landau damping octupoles and the uncertainty about the ultimate working area. In general, the beam covers up to seven 3rd and 4th order resonances right after RF trapping (largest tune spread), and their simultaneous compensation requires powering of at least 14 lenses.

New multipoles: number and types

The correction multipoles provided during Booster construction were conceived either for compensating specific stopbands in the working region $4.0 < Q_{H,V} < 5.0$ originally foreseen, or as an experimental tool in one ring, anticipating that more correction units may be needed[5]. Later it was realized that in particular skew sextupoles would be required for tackling $3Q_V = 16$, leading to a project for equipping the Booster with new multipoles[6]. The existing lenses were supplemented, in each ring, with 4 normal sextupoles (NS), 8 skew sextupoles (SS), 4 normal octupoles (NO), 8 skew octupoles (SO). They are combined in cylinders with concentric windings: "type A" contains NO, SO, NS, SS, and "type B" SO, SS. A summary of PSB correction multipoles from order 2 to 4 is given in Table 1.

Table 1: Non-zero harmonic correction multipoles (per ring): numbers, locations, strengths (in T for Normal and Skew Quadrupoles, T/m for NS, SS, T/m² for NO, SO).

Totals		"Old" multipoles			"New" multipoles			
	Type No.	in L1 [a] periods	in L3 [a] periods	Strength	in L1 [a] periods	Strength	in L4 [a] periods	Strength
NQ	8	3,8,11,16	4,8,12,16	0.05				
SQ	4		2,6,10,14	0.05				
NS	8	3,8,11,16	ANY [b]	2.05	4,6,9,12	2.25		
SS	8				4,6,9,12	2.3	2,6,11,12	3.0
NO	8	3,8,11,16		85	4,6,9,12	183.5		
SO	8				4,6,9,12	110	2,6,11,12	183.5

a) Straight sections L1: $\beta_H \sim 5.7$, $\beta_V \sim 2.7$; L3, L4: $\beta_H \sim 5.5$, $\beta_V \sim 12.5$.
b) By reconnecting chromaticity sextupoles in case of necessity.

As there is no conceivable situation where all 24 new lenses would be used at one time, 56(4 × 14) patchable supplies were provided. The larger number of multipoles and the flexibility for connecting them enables the user to select the best suited combinations with minimum repercussions on other stopbands.

Criteria for locating the lenses

General. Rather than designing a correction system around a given working point, all 3rd and 4th order resonances in the (accessible) area $4 < Q_H < 5$, $4 < Q_V < 5.5$ were considered. The system is laid out for i) single stopband compensation (implying pairs of lenses with phase relationship 90° [mod 180°] with respect to the harmonic involved, whenever possible), ii) simultaneous compensation of any two crossing 3rd order stopbands. Input data and boundary conditions were i) total number and types of existing lenses and of those to be installed; ii) PSB straight section occupation; iii) stopband characteristics computed from measured magnetic fields[7]; iv) typical experimental data[2,4].

Single stopbands. A total of 54 resonances of orders 3 and 4 are in the area considered. A simple formula derived from the 90° phase-shift criterion and applicable to any machine without superperiods helps to

select a hundred cases out of several hundred thousand possible locations. With

$$mQ_H + nQ_V = p \qquad (1)$$

(the harmonic p ranging from −12 to +22 in the PSB), ν the integer number of periods between any two lenses (supposed to be in identical lattice position), a phase shift of 90° (mod 180°) is provided if

$$\frac{\nu|p|}{p} = \frac{1}{4}\left(\bmod \frac{1}{2}\right), \quad \text{or} \quad \nu = \frac{4(\bmod 8)}{|p|} \qquad (2)$$

for P = 16 magnet periods. Note that Eq. (2) cannot be satisfied for |p| a multiple of eight. All other harmonics are readily covered by arranging four lenses (example: lenses in periods 2, 6, 11, 12) such as to dispose of lens pairs with

distance ν	odd	2,6	4
for harmonic |p|	4,12,20,...	2,6,10,14 ...	odd
example: periods	11-12	6-12	2-6.

Crossing points. No such simple rule is available for dealing with them. The strengths of the crossing stopbands m_1, n_1, p_1 and m_2, n_2, p_2, assuming that both are generated by skew sextupolar imperfections, are given by the cos and sin terms[8], $f_C^{p_1}$, $f_S^{p_1}$, $f_C^{p_2}$, $f_S^{p_2}$, respectively. Four SS with k_i lens strength per ampere are positioned at phases (with respect to the harmonic p considered) α_i^p and amplitude functions β_{Hi}, β_{Vi}, i = 1, ..., 4. The currents I_i have to satisfy

$$\begin{bmatrix} k_1\beta_{H_1}^{m_1/2}\beta_{V_1}^{n_1/2}\cos\alpha_1^{p_1} & \cdots\cdots & k_4\beta_{H_4}^{m_1/2}\beta_{V_4}^{n_1/2}\cos\alpha_4^{p_1} \\ k_1\beta_{H_1}^{m_1/2}\beta_{V_1}^{n_1/2}\sin\alpha_1^{p_1} & \cdots\cdots & k_4\beta_{H_4}^{m_1/2}\beta_{V_4}^{n_1/2}\sin\alpha_4^{p_1} \\ k_1\beta_{H_1}^{m_2/2}\beta_{V_1}^{n_2/2}\cos\alpha_1^{p_2} & \cdots\cdots & k_4\beta_{H_4}^{m_2/2}\beta_{V_4}^{n_2/2}\cos\alpha_4^{p_2} \\ k_1\beta_{H_1}^{m_2/2}\beta_{V_1}^{n_2/2}\sin\alpha_1^{p_2} & \cdots\cdots & k_4\beta_{H_4}^{m_2/2}\beta_{V_4}^{n_2/2}\sin\alpha_4^{p_2} \end{bmatrix} \begin{bmatrix} I_1 \\ I_2 \\ I_3 \\ I_4 \end{bmatrix} = \begin{bmatrix} f_C^{p_1} \\ f_S^{p_1} \\ f_C^{p_2} \\ f_S^{p_2} \end{bmatrix}$$

$$\text{or} \quad \{A\}\cdot\vec{I} = \vec{f}, \qquad (3)$$

in order to tackle both resonances. The determinant of {A} should be large to keep $\vec{I}$ small. For $p_1 \neq p_2$, solutions are straightforward as equations (in general) are linearly independent; for $p_1 = p_2$, equations are linearly dependent unless the lenses are located at very different β-values; this situation prevails around the main diagonal $Q_H = Q_V$, but does not apply to the present working area.

Final procedure. The criteria for selecting the lens arrangement amongst a hundred cases satisfying Eq. (2) were: i) with stopband strengths $\vec{f}$ from Ref. 7, choose the arrangement giving the smallest average lens current $\vec{I}$ for the 24 crossing points considered; ii) choose combinations that maximize the average value of the determinants [Eq. (3)]; iii) optimize on $3Q_V = 16$ and related crossing points. Actually, quite a few good solutions were obtained, and an arrangement convenient also for other reasons was finally selected. Criterion i) leads to the choice of power supplies with 150 A (data in Table 1 correspond to the lens rating of 270 A). Having all NS(NO) in positions with equal β-values may be a problem for a few crossing points, which may however be overcome by reconnecting a few zeroth harmonic NS not employed at present.

Results. The optimization procedure yielded a rather irregular pattern of lenses around the ring (Table 1). It is to be preferred to more conventional schemes (where lenses are positioned in opposite locations around the ring) if the system is intended to cover many resonances and their crossing points. Clearly a rearrangement of lenses may be envisaged at a later stage, for correcting a few stopbands more neatly.

Compensation of structural stopband $3Q_V = 16$: Results

Its features were investigated[9]: i) on a 70 MeV flat top, ii) during the first 100 ms of the acceleration cycle. A low intensity sample beam with a space-charge detuning of 0.01 provides a clean probing of the stopband. For studying its dynamic behaviour, the Q-tuning supplies were programmed to cross $3Q_V = 16$ rapidly at time t, which was varied in steps of 10 ms. For each case optimum compensation was found with the help of an automated scanning procedure[10]. Results are summarized in Fig. 2 and Table 2. The following
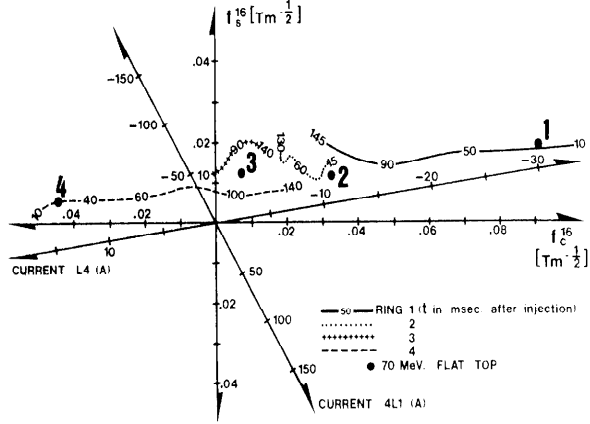

Fig. 2 Strength and phase of $3Q_V = 16$ during first 130 ms of cycle, derived from compensation settings.

features emerge: i) large stopband widths (> 0.01 in ring 1, complete beam loss in 5 ms); ii) considerable ring-to-ring differences, with marked dynamic (antisymmetric) behaviour of the outer rings 1 and 4; iii) 70 MeV flat top figures fit data found on the rising cycle after 30 ms, implying a negligible influence of dB/dt on $3Q_V = 16$. Also, even substantial closed orbit changes or Landau damping octupoles have little influence on this stopband: $\Delta|f^{16}| < 0.005$.

"Vertical emittance puzzle"

The speed of amplitude growth on a stopband depends on the initial emittance[8]. For $3Q_V = 16$, at PSB injection energy, and $\hat{\Delta}Q$ the peak incoherent tune variation due to the synchrotron motion, the number of stopband traversals N after which a particle is likely to be blown up from ϵ_V to A_V is

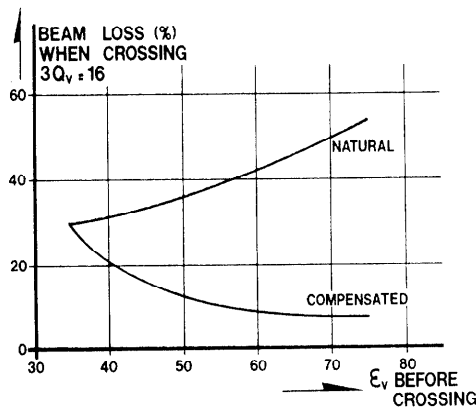$$N \approx 500 \frac{\hat{\Delta}Q(\sqrt{A_V/\epsilon_V} - 1)^2}{\epsilon_V|f^{16}|} \qquad (4)$$

Fig. 3 Vertical emittance puzzle. ϵ_V at 50 MeV.

3563

With non-perfect compensation ($f^{16} \neq 0$), fewer particles are expected to be lost for small ε_V; experimental data, however, appear to contradict this argument. Beam loss on crossing $3Q_V = 16$, as a function of ε_V before traversal, is plotted in Fig. 3: natural losses increase if ε_V is raised [as suggested by Eq. (4)], whereas residual losses go down, with the peculiar outcome that in order to achieve a useful degree of compensation, ε_V must be blown up, on purpose, right at injection. Beam profiles obtained by Beamscope[11] provide further evidence on this problem. Mechanisms possibly leading to this behaviour, but already eliminated by experiments, are : i) correction changes with ε_V; ii) correction changes during crossing time; iii) coherent transverse instabilities (sextupolar breathing mode); iv) redistribution of particles during traversal; v) faulty correction lenses or Q-tuning supplies; vi) dynamics related to the synchrotron motion; vii) dynamics related to space-charge effects (the ε_V-puzzle holds for 2×10^{11} up to 6×10^{12} pp ring).

Even with ε_V very large, complete compensation of $3Q_V = 16$ has never been achieved so far. It is felt that a mechanism of a different kind acts, like perhaps the structural 6th order stopband $6Q_V = 32$ generated by imperfection intrinsic to quadrupoles.

High dynamic working point

The tunes are $(Q_H, Q_V) = (4.30, 5.45)$ at injection[12], and are moved away from 3rd order stopbands as the Q-shift shrinks in the course of acceleration (Fig. 1). Programmed compensation of $3Q_V = 16$ (for 100 ms), $Q_H + 2Q_V = 15$(50 ms), $2Q_H + Q_V = 14$(20 ms) is required. The latter were studied on rising cycles, revealing that static compensation suffices during the time considered. 50 MeV stopband characteristics and widths $\Delta e = \Delta(mQ_H + nQ_V - p)$, for $\varepsilon_H^* = 33$, $\varepsilon_V^* = 20$ π μradm, are presented in Table 2 (computed strengths[7] are scaled from 800 to 50 MeV). Computed and measured data match fairly well in magnitude (except ring 1), confirming that the former were a valuable yard-stick for specifying the multipole system.

Table 2: Stopband strengths $f, d [10^{-3}$ Tm$^{-\frac{1}{2}}]$ and widths $\Delta e [10^{-3}]$ at 50 MeV (c = computed, m = measured)

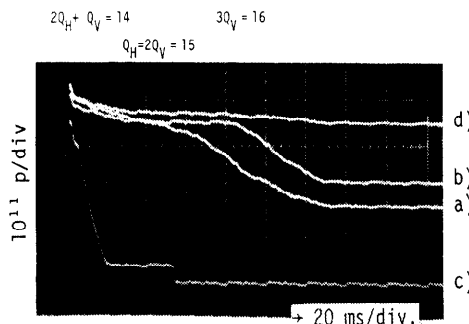| Ring	$3Q_V = 16$			$Q_H + 2Q_V = 15$			$2Q_H + Q_V = 14$		
	$\|f\|_c$	$\|f\|_m$	Δe_m	$\|d\|_c$	$\|d\|_m$	Δe_m	$\|f\|_c$	$\|f\|_m$	Δe_m
1	27	110	15.4	2.5	3	0.8	1.1	5.6	1.5
2	7	35	4.9	5.4	9	2.5	3.0	3.8	1.0
3	24	13	1.8	3.3	<2	<0.5	4.7	13.0	3.4
4	50	52	7.3	2.0	<2	<0.5	3.7	5.7	1.6

Fig. 4 Effect of stopbands and their compensation with the "high" dynamic working point, Ring 2. a) Natural loss; b) $Q_H + 2Q_V = 15$ compensated; c) 2-lens compensation of $3Q_V = 16$, thus fast loss on $2Q_H + Q_V = 14$; d) 4-lens correction of $3Q_V = 16$, $2Q_H + Q_V = 14$, plus b.

The single stopband data of $3Q_V = 16$ and $2Q_H + Q_V = 14$ yield f, and the four currents $\vec{I}$ providing simultaneous compensation are obtained by inverting Eq. (3); as $\vec{f}$ changes during acceleration for $3Q_V = 16$, $\vec{I}$ is a function of time as well. The effectiveness of this procedure is illustrated by Fig. 4, where a low-intensity beam follows the high dynamic working point in ring 2.

High intensity performance

A peak intensity of 1.7×10^{13} ppp has been accelerated so far on the high working point, compared to 1.8×10^{13} on the low one. In spite of this difference, due to imcomplete compensation and/or the mechanism leading to the "ε_V-puzzle", there is a marked increase in intensity passing through $\varepsilon_V^* = 15$ π μradm, prior to ejection, as demonstrated in Fig. 5. It is premature to set up the high working point in routine operation, but investigations towards mastering in particular the "ε_V-puzzle" are given high priority, as i) the new linac is likely to deliver even brighter beams; ii) $\bar{p}$ production implies vertical adding of 2×2 PSB beams at transfer to the PS[13], a technique demanding small vertical beam size because of the limited PS acceptance; iii) the ISR luminosity may profit from denser beams.
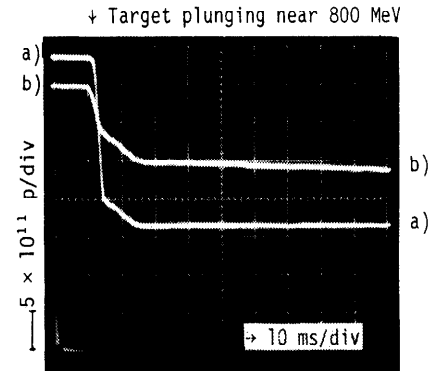

+ Target plunging near 800 MeV

Fig. 5 Increase of vertical beam density on the high working point b) as compared to the low one a). Target fork width $\varepsilon_V^* = 13$ π μradm.

References

1) E. Boltezar et al., this conf.
2) J. Gareyte et al., IEEE Trans. Nucl. Sci.
   Vol. NS-22, 855 (1975).
3) J.P. Delahaye, private communication.
4) J. Gareyte, CERN Int. Note MPS/DL/Note 74-3.
5) C. Bovet et al., Proc. 8th Intern. Conf. High-Energy Accel., CERN, Geneva, 1971, p. 380.
6) G. Baribaud et al., Int. Rep. CERN/PS/BR 77-42.
7) C. Bovet, K. Schindl, Int. Rep. CERN/SI/DL 70-4.
8) G. Guignard, CERN 70-24 (1970).
9) K. Schindl, E. Troianov, Int. Rep. CERN/PS-BR/78-16.
10) G. Metzger, private communication.
11) H. Schönauer, this conf.
12) J. Gareyte, P. Lefèvre, F. Sacherer, CERN Int. Note, MPS/DL/BR/Note 75-19.
13) J.P. Delahaye, P. Lefèvre, J.P. Riunaud, this conf.